*Bull. Pure Appl. Sci. Sect. E Math. Stat.*
**40E**(1), 45–59 (2021)
e-ISSN:2320-3226, Print ISSN:0970-6577
DOI 10.5958/2320-3226.2021.00005.9


**Bulletin of Pure and Applied Sciences**
**Section - E - Mathematics & Statistics**

Website : https : //www.bpasjournals.com/

# Study of couple stresses on MHD Poiseuille flow through a porous medium past an accelerated plate *

Raj Shekhar Prasad[1,†], Rajnish Kumar[2] and B.G. Prasad[3]

1. Department of Mathematics, Government Engineering College,
Buxar, Bihar, India.
2. Department of Mathematics, Birla Institute of Technology (Mesra),
Patna Campus, Patna-14, Bihar, India.
3. Department of Mathematics, Patna University,
Patna-4, Bihar, India.

1. E-mail: ✉ shekharraj.2010@gmail.com

2. E-mail: rajnish.bitpatna@gmail.com , 3. E-mail: profbgprasad@gmail.com

**Abstract** In this paper, we discuss an analytical study of the unsteady MHD flow of an incompressible electrically conducting couple stress fluid in the presence of porous medium between two parallel plates when the lower plate is accelerating while the upper plate is at rest, taking into account the pulsation of the pressure gradient effect and under the influence of a uniform magnetic field of strength $B_0$. The solution to the problem is obtained with the help of the perturbation technique. Analytical expressions are given for the velocity field, the shear stresses on the boundaries and the discharge between the plates and the effects of the various governing parameters entering into the problem are reported graphically to depict the interesting aspects of the solution.

**Key words** Couple stress, MHD, porous medium, accelerated plate.

**2020 Mathematics Subject Classification** 76D05, 76D10, 76S05, 76W05.

## Nomenclature of symbols

$x'$, Longitudinal coordinate;
$y'$, Transverse coordinate;
$u'$, Longitudinal velocity ;
$t'$, Time;
$P'$, Pressure;
$k$, Permeability of the medium;
$\mu$, Fluid viscosity;
$\rho$, Density of the fluid;
$\sigma$, Electric conductivity;

* Communicated, edited and typeset in Latex by *Lalit Mohan Upadhyaya* (Editor-in-Chief).
Received November 29, 2019 / Revised January 03, 2021 / Accepted February 04, 2021. Online First Published on June 30, 2021 at https://www.bpasjournals.com/.
†Corresponding author Raj Shekhar Prasad, E-mail: shekharraj.2010@gmail.com

$B_0$ ,Magnetic induction;
$\eta$, Coefficient of viscosity;
$A$, Acceleration of lower plate;
$h$, Distance between the plates;
$u$, Dimensionless longitudinal velocity;
$t$, Dimensionless time;
$P$, Dimensionless pressure;
$x$, Dimensionless longitudinal coordinate;
$y$, Dimensionless transverse coordinate;
$a$, Couple stress parameter;
$\nu$, Kinematic viscosity;
$R_e$, Reynolds number;
$L$, Material constant $\left(\sqrt{\frac{\eta}{\mu}}\right)$;
$M$, Hartmann number;
$K$, Darcy parameter;
$P_s$, Amplitude of pulsation (steady part);
$P_0$, Amplitude of pulsation (unsteady part);
$u_s$, Steady part of velocity $u$;
$u_0$, Unsteady part of velocity $u$;
$\omega$, Pulsation frequency;
$Q$, Discharge between the plates;
$\tau_L$, Shear stress on the lower plate;
$\tau_W$, Shear stress on the upper plate;

## 1 Introduction

Research on couple stress fluids has attracted the attention of research workers in fluid mechanics during the last four decades. The couple stress fluid may be considered as a special case of non-Newtonian fluid. The main characteristics of this fluid is to introduce a size dependent effect. The theory of couple stress fluids, introduced by Stokes [25], have distinct features, such as the presence of couple stresses, body couples and the non-symmetric stress tensor. The detailed study of this theory is given in the monograph of Stokes [27]. The analytical and computational studies of diverse couple stress fluid flows dealing with a class of axi-symmetric problems are studied by Rao and Iyengar [22]. The research on couple stress fluids has several industrial and scientific applications such as the extrusion of polymer fluids, solidification of liquid crystals, cooling of a metallic plate in a bath, the colloidal solutions, the dynamics of synovial fluid present in the synovial joints and the theory of lubrication (e.g., see Naduvinamani et al. [15–19], Lin and Hung [9]).

For couple stress fluids, a number of studies are carried out earlier owing to its widespread industrial and scientific applications. Some relevant works are those of Stokes [26], Ramanaih [21], Bujurke and Naduvinami [2], Gupta and Sharma [6], Mokhiamer et al. [14], Li-Wang et al. [10] and many others. The couple stress fluids are the fluids consisting of rigid, randomly oriented particles suspended in a viscous medium, such as the blood, lubricants containing a small amount of high polymer additive, electro-rheological fluids and the synthetic fluids. The main feature of the couple stress fluids is that the stress tensor is anti-symmetric and their accurate flow behavior cannot be predicted by the classical Newtonian theory. Stokes [26] generalized the classical model to include the effect of the presence of the couple stresses and this couple stress fluid model has since then been widely used because of its relative mathematical simplicity as compared to the other models developed for the couple stress fluids.

Many authors [1, 3, 5, 8, 12, 13] have studied the effects of couple stresses on flow past an infinite plate or past a sphere and through channels for constant or absent pressure gradient (e.g., Annapurna and Ramanaiah [1], Chaturani [3], Mindlin and Tierstea [13], Stokes [27], etc.), while in the absence of an effect of couple stress, Edwards et al. [5], discussed the pulsating flow of non-Newtonian fluids in pipes. Also, the oscillatory fluid flow through a porous medium channel bounded by two impermeable parallel plates was studied by Khodadadi [8]. Some of the recent developments in this area are Makinde and Eegunjobi [11], Rudraiah et al. [23], Kaladhar et al. [7] and Sarojini et al. [24].

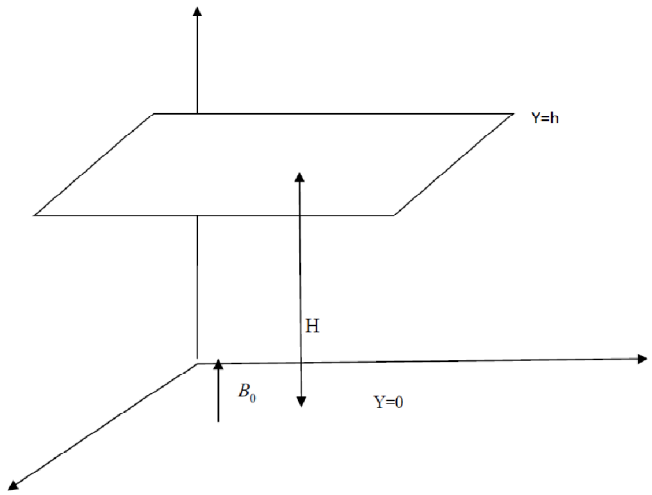


Fig. 1: The governing model of the problem.

During the recent years, considerable attention has been given to the pulsatile flows of fluids in channels or tubes of various cross-sections due to its rapid expanse and widespread industrial, environmental and physiological applications. The pulsating flow is of practical importance in Biology (e.g., in heart beating), heat transfer enhancement and automotive industry (simulation of exhaust from internal combustion engines).

The analysis in the present work is an extension of work by Nabil et al. [4] and Prasad and Prasad [20]. Some of the applications related to this idea are the flow of oil underground where there is a natural magnetic field, and the motion of blood through the arteries. The main idea of our work is the mathematical study of these phenomena, and our purpose is to show the relation between the different parameters of the motion of the external forces, to investigate how to control the velocity of fluid motion by changing these parameters and external forces.

The main intend of our work is to study the effects of couple stresses, pressure pulsation, and magnetic parameters on the velocity distribution of an incompressible, electrically conducting fluid through porous media flowing between two parallel plates channel, where the lower plate is accelerated. The solution of the problem is obtained with the help of the perturbation technique. Analytical expressions are given for the velocity field, the non-dimensional discharge between the plates and the wall shear, and the effects of the various parameters entering into the problem are discussed with the help of graphs.

## 2 Mathematical formulation of the problem

We consider the unsteady MHD flow of couple stress fluid through a porous medium induced by the pulsation of the pressure gradient. The plates are assumed to be electrically insulated. We choose a Cartesian co-ordinate system $O\,(x',\, y'\,,\, z')$ such that the boundary walls are at $y' = 0$ and $y' = h$ and they are assumed to be parallel to the $x'z'$-plane. Here the lower boundary wall at $y' = 0$ is taken as an accelerated plate while the upper wall at $y' = h$ is at rest. A uniform magnetic field of strength $B_0$ is acting along the $y'$-axis. The induced magnetic field is assumed to be negligible. The governing momentum equations from the Navier-Stokes equation can be shown (see, [4]) in the following form for the above flow regime:

For incompressible fluids $\nabla.v = 0$, then, if the body force $f$ and the body moment $I$ are absent, the

equation of motion reduces to

$$\frac{\partial u'}{\partial t'} = -\frac{1}{\rho}\frac{\partial P'}{\partial x'} + \frac{\mu}{\rho}\frac{\partial^2 u'}{\partial y'^2} - \frac{\eta}{\rho}\frac{\partial^4 u'}{\partial y'^4} - \frac{\sigma B_0^2 u'}{\rho} - \frac{\mu}{\rho k}u'. \tag{2.1}$$

Here the term $-\frac{\eta}{\rho}\frac{\partial^4 u'}{\partial y'^4}$ in the above equation gives the effect of couple stresses, while $\frac{-\sigma B_0^2 u'}{\rho}$ signifies the electromagnetic force and the term $\frac{-\mu}{\rho k}u'$ occurs due to porous media. All the physical variables in the above equation have their usual meaning.
Since the plate at $y' = 0$ is accelerating while the upper plate $y' = h$ is at rest, therefore the boundary conditions corresponding to the problem under consideration are

$$u' = At' \text{ at } y' = 0, \tag{2.2}$$

$$u' = 0 \quad \text{at} \quad y' = h. \tag{2.3}$$

Further the couple stresses vanish at both the plates, therefore, we have

$$\frac{\partial^2 u'}{\partial y'^2} = 0 \text{ at } y' = 0, \tag{2.4}$$

and

$$\frac{\partial^2 u'}{\partial y'^2} = 0 \text{ at } y' = h, \tag{2.5}$$

where $u'(y', t')$ is the fluid velocity field and $h$ is the distance between the two plates.

## 3 Non-dimensionalization

We introduce the following dimensionless quantities

$$\begin{aligned} &u = \frac{u'}{(A\nu)^{\frac{1}{3}}}, t = t'\left(\frac{A^2}{\nu}\right)^{\frac{1}{3}}, P' = A\rho h P, x' = xh; y' = yh, a^2 = {h^2}/{L^2}, \\ &L^2 = \frac{\eta}{\mu}, R_e = \left(\frac{A^2}{\nu}\right)^{\frac{1}{3}}\frac{\rho h^2}{\mu}, \eta = \frac{\rho h^4}{(A\nu)^{\frac{1}{3}}}, M^2 = \frac{B_0^2\sigma h^2}{\mu}, \frac{1}{K} = \frac{h^2}{k} \end{aligned} \tag{3.1}$$

in (2.1) and the boundary conditions (2.2) - (2.5) to get

$$R_e a^2\frac{\partial u}{\partial t} = -R_e a^2\frac{\partial P}{\partial x} + a^2\frac{\partial^2 u}{\partial y^2} - \frac{\partial^4 u}{\partial y^4} - a^2\left(M^2 + \frac{1}{K}\right)u. \tag{3.2}$$

The boundary conditions in non-dimensional form are

$$\begin{aligned} &u = t, && u'' = 0 && \text{at} && y = 0; \\ &u = 0, && u'' = 0 && \text{at} && y = 1. \end{aligned} \tag{3.3}$$

All the physical variables are defined in the nomenclature. The solutions are obtained for hydro magnetic flow field in the presence of couple stresses, porous medium and pulsation of pressure gradient.

## 4 Mathematical solution of the problem

For the pulsation of the pressure gradient we have

$$-\frac{\partial P}{\partial x} = \left(\frac{\partial P}{\partial x}\right)_s + \left(\frac{\partial P}{\partial x}\right)_o e^{i\omega t}. \tag{4.1}$$

Then (3.2) reduces to the form

$$R_e a^2\frac{\partial u}{\partial t} = R_e a^2\left[\left(\frac{\partial P}{\partial x}\right)_S + \left(\frac{\partial P}{\partial x}\right)_o e^{i\omega t}\right] + a^2\frac{\partial^2 u}{\partial y^2} - \frac{\partial^4 u}{\partial y^4} - a^2\left(M^2 + \frac{1}{K}\right)u. \tag{4.2}$$

Now (4.2) can be solved by using the following perturbation technique

$$u = u_s + u_o e^{i\omega t}. \tag{4.3}$$

Using (4.3) in (4.2) and (3.3) and equating the like terms on both the sides, we get the following system of equations:

$$\frac{d^4u_s}{dy^4} - a^2\frac{d^2u_s}{dy^2} + a^2\left(M^2 + \frac{1}{K}\right)u_s = R_e a^2 P_S, \tag{4.4}$$

$$\frac{d^4u_o}{dy^4} - a^2\frac{d^2u_o}{dy^2} + a^2\left(M^2 + \frac{1}{K} + R_e i\omega\right)u_o = R_e a^2 P_O. \tag{4.5}$$

The boundary conditions (2.3) lead to

$$\begin{array}{llll} u_s = t, & u_0 = 0, & \text{at} & y = 0, \\ u_s'' = 0, & u_0'' = 0, & \text{at} & y = 0, \\ u_s = 0, & u_0 = 0, & \text{at} & y = 1, \\ u_s'' = 0, & u_0'' = 0, & \text{at} & y = 1. \end{array} \tag{4.6}$$

The solution of (4.4) and (4.5) subject to the boundary conditions (4.6) gives the velocity distribution of the fluid under consideration and the solution is derived as follows

$$\begin{aligned} u = &\left(-N_9 e^{\lambda_1 y} + N_8 e^{\lambda_2 y} + N_7 e^{\lambda_3 y} + N_6 e^{\lambda_4 y} + \frac{R_e P_S}{\left(M^2 + \frac{1}{K}\right)}\right) \\ &+ \left[-N_{19} e^{\lambda_5 y} + N_{18} e^{\lambda_6 y} + N_{17} e^{\lambda_7 y} + N_{16} e^{\lambda_8 y} + \frac{R_e P_O}{\left(M^2 + \frac{1}{K} + R_e i\omega\right)}\right] e^{i\omega t}. \end{aligned} \tag{4.7}$$

where $\lambda_1$–$\lambda_8$ and $N_1$–$N_{19}$ are given in the Appendix at the end of the paper.
The non-dimensional discharge between the plates per unit depth is given by $Q$, where,

$$\begin{aligned} Q &= \int_0^1 u\,(y,t)dy \\ &= \left[-\frac{N_9}{\lambda_1}(e^{\lambda_1} - 1) + \frac{N_8}{\lambda_2}(e^{\lambda_2} - 1) + \frac{N_7}{\lambda_3}(e^{\lambda_3} - 1) + \frac{N_6}{\lambda_4}(e^{\lambda_4} - 1) + \frac{R_e P_S}{\left(M^2 + \frac{1}{K}\right)}\right] \\ &+ \left[-\frac{N_{19}}{\lambda_5}(e^{\lambda_5} - 1) + \frac{N_{18}}{\lambda_6}(e^{\lambda_6} - 1) + \frac{N_{17}}{\lambda_7}(e^{\lambda_7} - 1) + \frac{N_{16}}{\lambda_8}(e^{\lambda_8} - 1) + \frac{R_e P_O}{\left(M^2 + \frac{1}{K} + R_e i\omega\right)}\right] e^{i\omega t}. \end{aligned} \tag{4.8}$$

The shear stresses on the lower and upper plates are given in dimensionless form as

$$\begin{aligned} \tau_L = \left(\frac{du}{dy}\right)_{y=0} = &\left[-N_9\lambda_1 + N_8\lambda_2 + N_7\lambda_3 + N_6\lambda_4\right] + \\ &\left[-N_{19}\lambda_5 + N_{18}\lambda_6 + N_{17}\lambda_7 + N_{16}\lambda_8\right] e^{i\omega t}, \end{aligned} \tag{4.9}$$

$$\begin{aligned} \tau_W = \left(\frac{du}{dy}\right)_{y=1} = &\left[-N_9\lambda_1 e^{\lambda_1} + N_8\lambda_2 e^{\lambda_2} + N_7\lambda_3 e^{\lambda_3} + N_6\lambda_4 e^{\lambda_4}\right] + \\ &\left[-N_{19}\lambda_5 e^{\lambda_5} + N_{18}\lambda_6 e^{\lambda_6} + N_{17}\lambda_7 e^{\lambda_7} + N_{16}\lambda_8 e^{\lambda_8}\right] e^{i\omega t}. \end{aligned} \tag{4.10}$$

## 5 Results and discussion

The effect of the significant parameters of the problem on the velocity, discharge and skin-friction are illustrated graphically in Fig. 2 – Fig. 15. Fig. 2 and Fig. 3 exhibit the effect of pulsation $P_0$ on the velocity for $R_e = 2$ and $R_e = 20$ respectively. We find that an increase in $P_0$ leads to a decrease in the velocity. For $R_e = 2$ the velocity profiles are almost linear for all values of $P_0$ whereas for $R_e = 20$ the profiles become asymptotic.
Fig. 4, Fig. 5 and Fig. 6 reveal the influence of the porosity parameter $K$ for distinct values of the Reynolds number $R_e$. As $K$ increases from 0.001 to 1, the velocity increases. Moreover for a fixed value of $K$ and $R_e = 2$ and $R_e = 20$ the velocity decreases when $y$ increases from 0 to 1, but for $R_e = 50$ and $K = 0.01, 0.1$ and 1 the velocity increases initially and after achieving its maximum value the velocity decreases with the increment in $y$.
Fig. 7 shows the effect of Hartmann number $M$on the velocity profiles. As expected, velocity decreases with the increment in $M$.
Fig. 8 illustrates that the effect of the couple stress is to increase the velocity with increasing stress. It can be observed that with the increment in $a$ the velocity decreases initially with the initial values

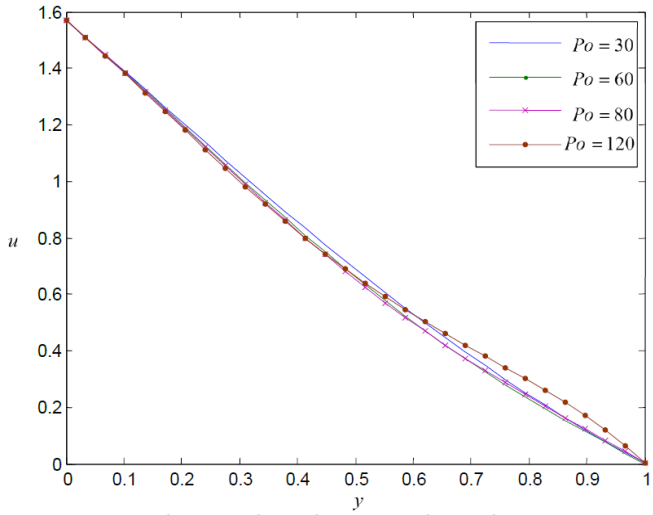


Fig. 2: Velocity distribution plotted versus position for $M = 5$, $a = 0.5, K = 0.1, \omega = 1$, $P_s = 5$, $t = \pi/2$ , $R_e = 2$.

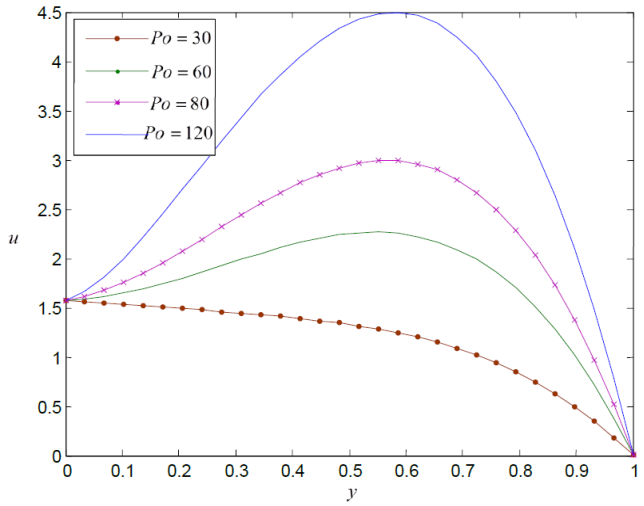


Fig. 3: Velocity distribution plotted versus position for $M = 5$, $a = 0.5, K = 0.1, \omega = 1$, $P_s = 5$, $t = {}^{\pi}/_{2}$ , $R_e = 20$.

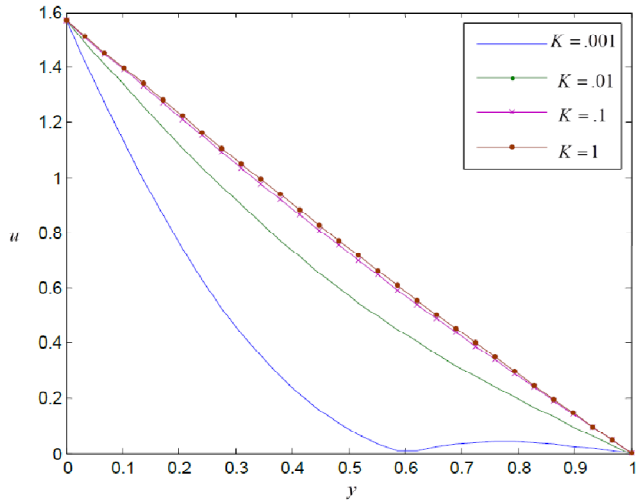


Fig. 4: Velocity distribution plotted versus position for $M = 5$, $a = 0.5, \omega = 1$, $P_s = 5$, $P_o = 5, t = \pi/2$ , $R_e = 2$.

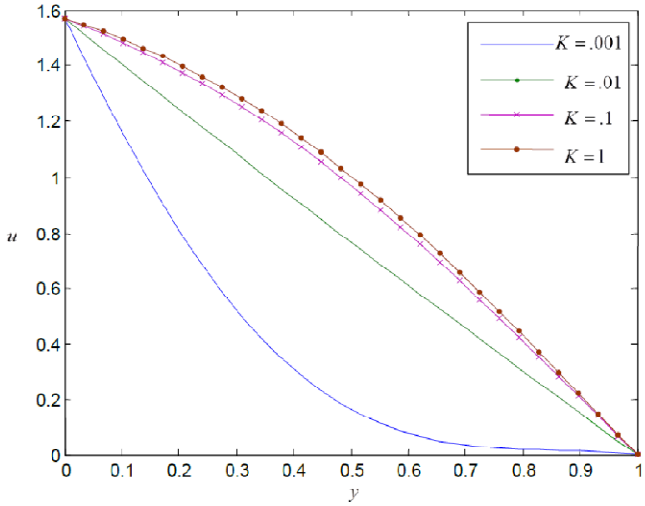


Fig. 5: Velocity distribution plotted versus position for $M = 5$, $a = 0.5, \omega = 1$, $P_s = 5, P_o = 5$, $t = \pi/2$ , $R_e = 20$.

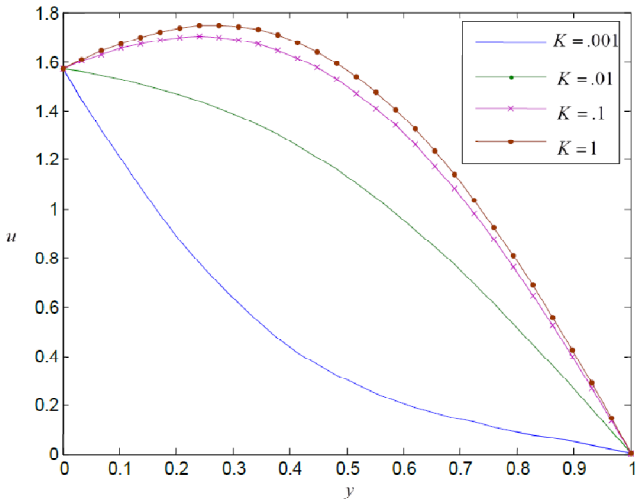


Fig. 6: Velocity distribution plotted versus position for $M = 5$, $a = 0.5, \omega = 1$, $P_s = 5, P_o = 5$, $t = \pi/2$ , $R_e = 50$.

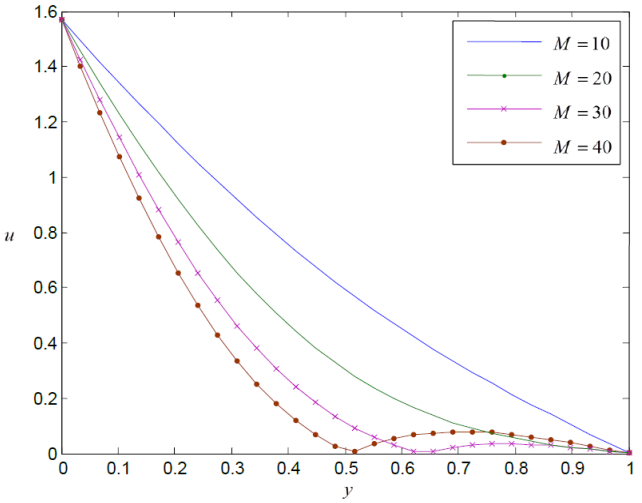


Fig. 7: Velocity distribution plotted versus position for $K = 0.1$, $a = 0.5, \omega = 1$, $P_s = 5, P_o = 5$, $t = \pi/2$ , $R_e = 2$.

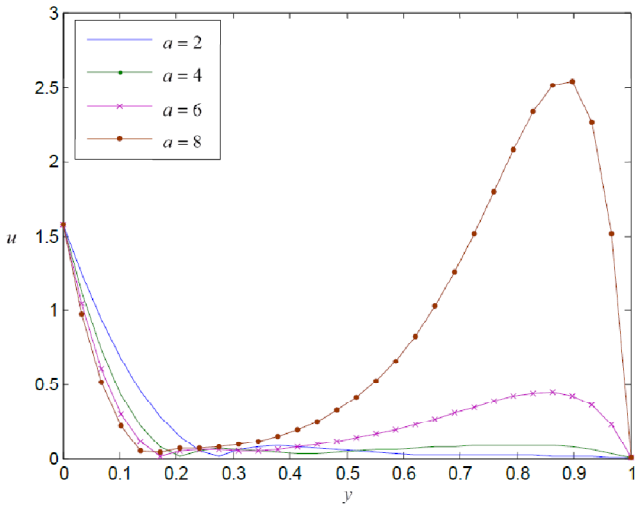


Fig. 8: Velocity distribution plotted versus position for $K = 0.1$, $M = 40, \omega = 1$, $P_s = 5, P_o = 5$, $t = \pi/2$ , $R_e = 2$.

of $y$ and then it increases with the increment in $a$. The effects of pulsation frequency $\omega$ on the velocity profiles are exhibited in Fig. 2 – Fig. 11. The velocity increases when $\omega$ varies from 5 to 10 but when $\omega$ increases from 10 to 20 a considerable enhancement in the velocity distribution occurs. For all values of $\omega$, the velocity decreases with the increment in $y$. Also for all values of $\omega$, $K = 0.1, 0.01$ and $R_e = 2, 20$ the maximum velocity can be found as approximately 1.6 and its minimum value as 0.
Fig. 12 and Fig. 13 depict the discharge, i.e., the mass flux flow $Q$ against $M$ for various values of the pertinent parameters. The discharge $Q$ increases with the increment in $K$ and it increases when $K = 0.1$ and $K = 0.01$, except for $R_e = 2$, and when $M$ varies from 1 to 3. Moreover when $R_e = 50$ the discharge remains constant for $K = 0.001$ and for $K = 0.01$ with the increment in $M$.
In order to investigate the influence of the porosity parameter $K$ on the Skin-friction on the plates we have presented the values of the Skin-friction. In Fig. 14 and Fig. 15 we observe that for $R_e = 2$ and $R_e = 50$ the Skin-friction increases initially as $K$ increases and it decreases for all values of $K$ when $M$ exceeds 1.5 and after attaining the minimum value at $M = 1.58$ (approx.), it starts to increase again. Also at this stage the Skin-friction has equal values for all $K$. When $R_e = 50$, the Skin-friction increases as $K$ varies from 0.1 to 10 but it remains constant when $K = 0.001$ and $K = 0.01$. When the porosity parameter $K$ tends to infinity the results agree with the corresponding ones of Nabil et al. [4].

## 6 Conclusions

The effect of couple stresses on MHD Poiseuille flow through a porous medium past an accelerated plate is investigated in this paper. The exact expressions for the velocity, the non-dimensional discharge and the wall shear at the upper plate are obtained analytically. Graphical results are presented for the velocity with the variation of pulsation $P_0$, the Hartmann number $M$, the couple stress parameter $a$, the amplitude of the pulsation of the pressure gradient $\omega$ and the porosity parameter $K$ and for the non-dimensional discharge and the wall shear with variation of porosity parameter $K$.
The main findings can be summarized as follows:
1. The magnitude of the velocity reduces with the increase in pulsation $P_0$ and the Hartmann number $M$, whereas the velocity increases with increase in the couple stress parameter $a$ and the amplitude of the pulsation of the pressure gradient $\omega$.
2. The magnitude of the velocity on either plate enhances with the increase in the porosity parameter $K$.

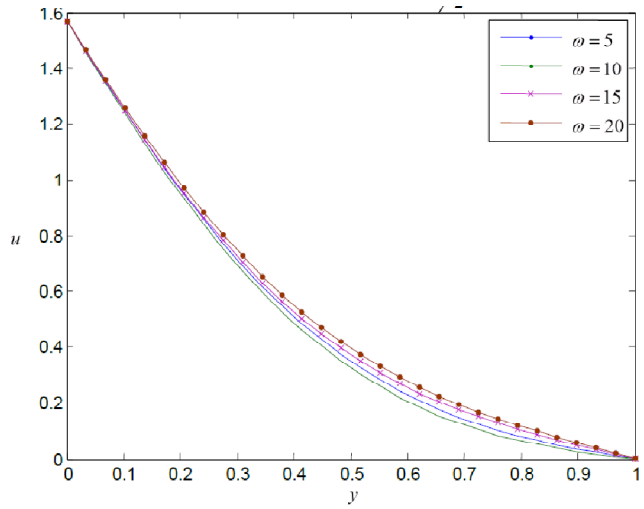


Fig. 9: Velocity distribution plotted versus position for $K = 0.1$, $M = 10, a = 1$, $P_s = 5, P_o = 5$, $t = \pi/2$ , $R_e = 2$.

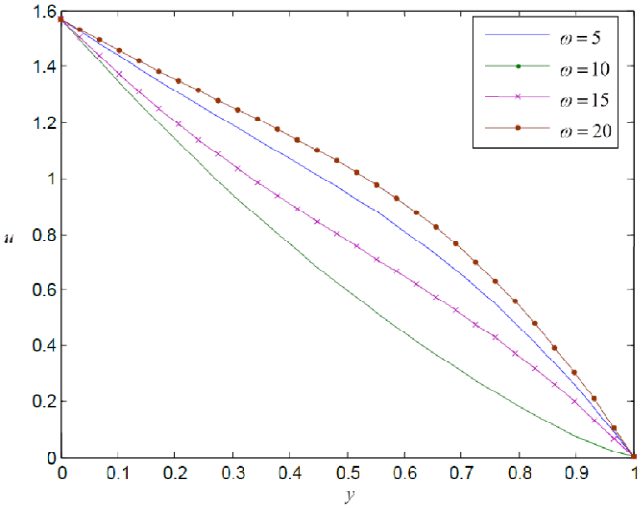


Fig. 10: Velocity distribution plotted versus position for $K = 0.1$, $M = 10, a = 1$, $P_s = 5, P_o = 5$, $t = \pi/2$ , $R_e = 20$.

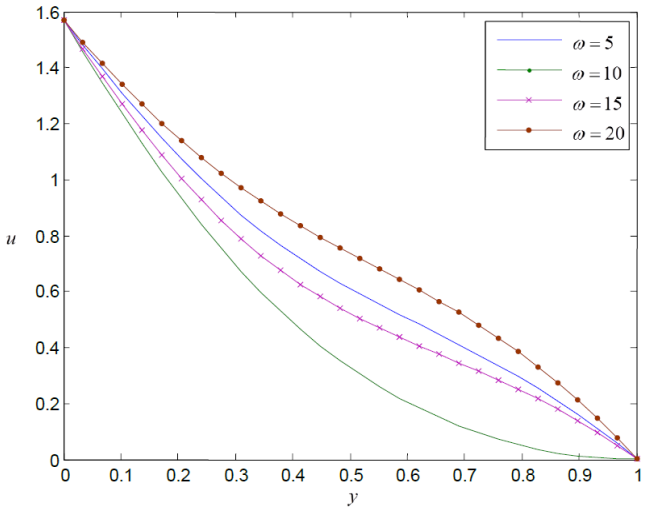


Fig. 11: Velocity distribution plotted versus position for $K = 0.01,\ M = 10, a = 1,\ P_s = 5, P_o = 5,\ t = \pi/2\ ,\ R_e = 20.$

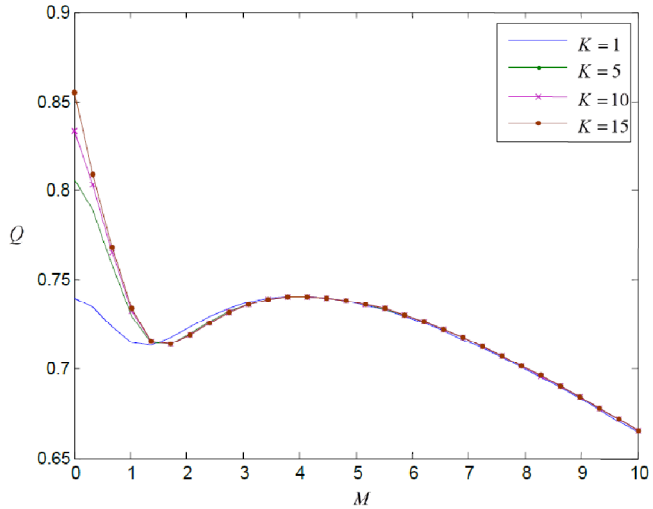


Fig. 12: The discharge $Q$ plotted versus $M$ for $P_o = 20,\ a = 0.5,\ P_s = 5,\ t = \pi/2,\ R_e = 2, \omega = 1.$

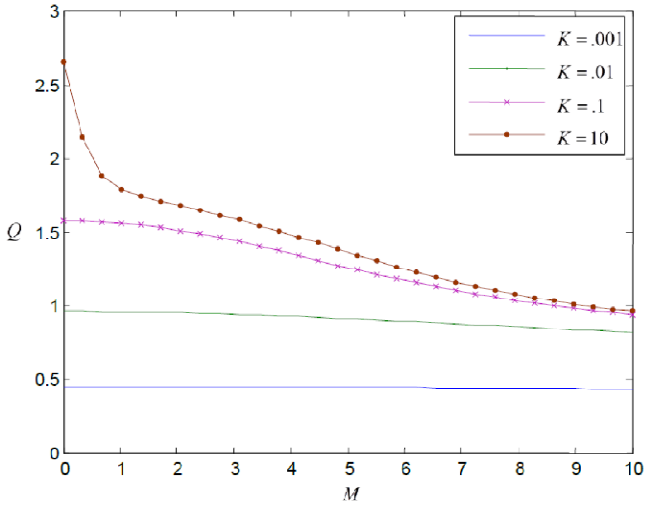


Fig. 13: The discharge $Q$ plotted versus $M$ for $P_o = 20,\ a = 0.5,\ P_s = 5,\ t = \pi/2,\ R_e = 50, \omega = 1$.

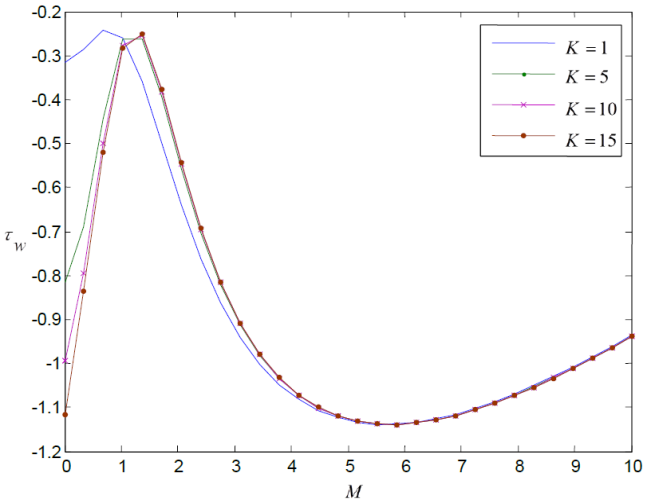


Fig. 14: The Skin friction $\tau_w$ plotted versus $M$ for $P_o = 20,\ a = 0.5,\ P_s = 5,\ t = \pi/2,\ R_e = 2, \omega = 1$.

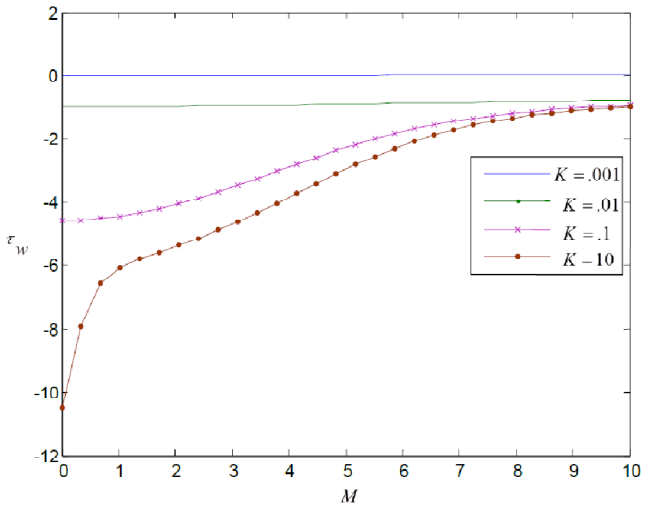


Fig. 15: The Skin friction $\tau_w$ plotted versus $M$ for $P_o = 20$, $a = 0.5$, $P_s = 5$, $t = \pi/2$, $R_e = 50, \omega = 1$.

3. The discharge $Q$ increases with the increment in the porosity parameter $K$.
4. The Skin friction $\tau_w$ on the upper plate $y' = h$ increases with the increase in the porosity parameter $K$.

**Acknowledgments** The authors express their gratitude to the referees and to the Editor-in-Chief for suggesting modifications and corrections in the original draft of this paper which have upgraded this manuscript.

## References

[1] Annapurna, N. and Ramaniah, G. (1976). Effect of couple stresses on the unsteady drainage of a micro-polar fluid on a flat surface , *Jpn. J. Appl. Phys.*, 15, 2441–2444.

[2] Bujurke, N.M. and Naduvinamani, N.G. (1990). The lubrication of lightly cylinders in combined rolling, sliding and normal motion with couple stress fluid , *Int. J. Sci.*, 32, 969–979.

[3] Chaturani, P. (1978). Viscosity of Poiseuille flow of a couple stress fluid with applications to blood flow, *Biorheology*, 15, 119–128.

[4] Nabil, T.M., El-Dabe, Salba and Mohandis, M.G. (1965). Effect of couple stresses on pulsatile hydromagnetic Poiseuille flow, *Fluid Dynamics Research*, 15(5), 313–324.

[5] Edwards, M.F., Nelist, D.A. and Wilkinson, W.L. (1972). Pulsating flow of non-Newtonian fluids in pipes, *Chem. Engg. Sc.*, 27, 545–553.

[6] Gupta, R.S. and Sharma, R.L. (1988). Analysis of couple stresses lubricant in hydrostatic thrust bearings, *Wear.*, 48, 257–269.

[7] Kaladhar, K., Motsa S.S. and Srinivasacharya, D. (2016). Mixed convection flow of couple stress fluid in a vertical channel with radiation and Soret effects, *Journal of Applied Fluid Mechanics*, 9(1), 43–50.

[8] Khodadadi, J.M. (1991). Oscillatory fluid flow through a porous medium channel bounded by two impermeable parallel plates, *J. Fluids Engg.*, 133, 509–511.

[9] Lin, J.R. and Hung, C.R. (2007). Combined effects of non- Newtonian couple stresses and fluid inertia on squeeze film characteristics between a long cylinder and an infinite plate, *Fluid Dyn. Res.*, 39(8), 616–639.

[10] Li-Wang, Qin-zhu and Zhu-Wen (2002). On the performance of dynamically loaded journal bearings with couple stresses fluids, *Tribology Int.*, 35, 185–191.

[11] Makinde, O.D. and Eegunjobi, A.S. (2013). Entropy generation in a couple stress fluid flow through a vertical channel filled with saturated porous media, *Entropy*, 15, 4589–4606. doi:10.3390/e15114589.

[12] Mindlin, R.D. (1973). Influence of couple stresses in linear elasticity, *Exp. Mech.*, 20, 1–7.

[13] Mindlin, R.D. and Tierstea, H.F. (1962). Effects of couple stresses in linear elasticity, *Arch. Ration. Mech. Anal.*, 11, 415–448.

[14] Mokhiamer, U.M., Crosby, W.A. and El-Gamel, H.A. (1999). A study of journal bearing lubricated by fluids with couple stresses considering the elasticity of the liner, *Wear.*, 224, 194–201.

[15] Naduvinamani, N.B., Hiremath, P.S. and Gurubasavaraj, G. (2005). Effects of surface roughness on the couple stress squeeze film between a sphere and a flat plate, *Tribol. Int.*, 38(5), 451–458.

[16] Naduvinamani, N.B., Hiremath, P.S. and Gurubasavaraj, G. (2002). Surface roughness effects in a short porous journal bearing with couple stress fluid, *Fluid Dyn. Res.*, 31(5-6), 333–354.

[17] Naduvinamani, N.B., Hiremath, P.S. and Gurubasavaraj, G. (2001). Squeeze film lubrication of a short porous journal bearing with a couple stress fluids, *Tribol. Int.*, 34(11), 739–747.

[18] Naduvinamani, N.B., Fatima, S.T. and Hiremath, P.S. (2003). Effect of surface roughness on characteristics of couple stress squeeze film between an isotropic porous rectangular plates, *Fluid Dyn. Res.*, 32(5), 217–231.

[19] Naduvinamani, N.B., Fatima, S.T. and Hiremath, P.S. (2003). Hydromagnetic lubrication of rough slider bearing with couple stress fluids, *Tribol. Int.*, 36 (12), 949–959.

[20] Prasad R.S. and Prasad, B.G. (2012). Study of couple stress fluid through porous medium in a parallel plate channel, *IOSR Journal of Mathematics*, 4(2), 10–17.

[21] Ramanaiah, G. (1979). Squeeze films between finite plates lubricated by fluids with couple-stresses, *Wear.*, 54, 315–320.

[22] Rao Lakshman, S.K. and Iyengar, T.K.V. (1985). Analytical and computational studies in couple stress fluids flows, UGC Research project: C-8-482, SR-III. (This project was sanctioned at the Department of Mathematics, National Institute of Technology, Warangal 506 004, India.)

[23] Rudraiah, N., Shankar B.M. and Ng, C.O. (2011). Electrohydromagnetic stability of couple stress fluid in a channel occupied by a porous medium, *Special Topics and Reviews in Porous Media*, 2(1), 11–22.

[24] Sarojini, M.S., Krishna, M.V. and Uma Shankar, C. (2011). MHD flow of couple stress fluid through a porous medium in a parallel plate channel in presence of effect of inclined magnetic field, *International Journal of Physics and Mathematical Sciences*, 1(1), 9–18.

[25] Stokes, V.K. (1966). Couple stresses in fluids, *Phys. Fluids*, 9, 1709–1715.

[26] Stokes, V.K. (1971). Effects of couple stresses in fluids on the creeping flow past a sphere, *Phys. Fluids.*, 14, 1580–1582.

[27] Stokes, V.K. (1984). Theories of fluids with Microstructure, Springer, New York.

**Appendix**

$$\lambda_1 = \left[\frac{1}{2}\left(a^2 + \left(a^4 - 4a^2\left(M^2 + \frac{1}{K}\right)\right)^{\frac{1}{2}}\right)\right]^{\frac{1}{2}}, \lambda_2 = -\lambda_1, \tag{A.1}$$

$$\lambda_3 = \left[\frac{1}{2}\left(a^2 - \left(a^4 - 4a^2\left(M^2 + \frac{1}{K}\right)\right)^{\frac{1}{2}}\right)\right]^{\frac{1}{2}}, \lambda_4 = -\lambda_3, \tag{A.2}$$

$$\lambda_5 = \left[\frac{1}{2}\left(a^2 + \left(a^4 - 4a^2\left(M^2 + \frac{1}{K} + R_e i\omega\right)\right)^{\frac{1}{2}}\right)\right]^{\frac{1}{2}}, \lambda_6 = -\lambda_5, \tag{A.3}$$

$$\lambda_7 = \left[\frac{1}{2}\left(a^2 - \left(a^4 - 4a^2\left(M^2 + \frac{1}{K} + R_e i\omega\right)\right)^{\frac{1}{2}}\right)\right]^{\frac{1}{2}}, \lambda_8 = -\lambda_7, \tag{A.4}$$

$$\left(\frac{\partial P}{\partial x}\right)_s = P_S, \left(\frac{\partial P}{\partial x}\right)_o = P_O, \tag{A.5}$$

$$N_0 = (e^{\lambda_1} - e^{\lambda_3})(\lambda_2^2 - \lambda_3^2), N_1 = (e^{\lambda_1} - e^{\lambda_4})(\lambda_2^2 - \lambda_4^2), \tag{A.6}$$

$$N_2 = \left[\frac{R_e P_S}{\left(M^2 + \frac{1}{K}\right)}(e^{\lambda_1} - 1)\lambda_2^2 - te^{\lambda_1}\right]\lambda_2^2, \tag{A.7}$$

$$N_3 = (\lambda_1^2 e^{\lambda_2} - \lambda_2^2 e^{\lambda_1})(\lambda_1^2 e^{\lambda_1} - \lambda_3^2 e^{\lambda_3}) - (\lambda_1^2 e^{\lambda_3} - \lambda_3^2 e^{\lambda_1})(\lambda_1^2 e^{\lambda_1} - \lambda_2^2 e^{\lambda_2}), \tag{A.8}$$

$$N_4 = (\lambda_1^2 e^{\lambda_1} - \lambda_4^2 e^{\lambda_4})(\lambda_1^2 e^{\lambda_2} - \lambda_2^2 e^{\lambda_1}) - (\lambda_1^2 e^{\lambda_4} - \lambda_4^2 e^{\lambda_1})(\lambda_1^2 e^{\lambda_1} - \lambda_2^2 e^{\lambda_2}), \tag{A.9}$$

$$N_5 = \left[\frac{R_e P_S}{\left(M^2 + \frac{1}{K}\right)}(e^{\lambda_1}(\lambda_1^2 e^{\lambda_2} - \lambda_2^2 e^{\lambda_1}) - (\lambda_1^2 e^{\lambda_1} - \lambda_2^2 e^{\lambda_2})) - te^{\lambda_1}(\lambda_1^2 e^{\lambda_2} - \lambda_2^2 e^{\lambda_1})\right]\lambda_1^2, \tag{A.10}$$

$$N_6 = \frac{N_5 N_0 - N_2 N_3}{N_1 N_3 - N_4 N_0}, \; N_7 = \frac{N_2 N_4 - N_1 N_5}{N_1 N_3 - N_0 N_4}, \tag{A.11}$$

$$N_8 = \frac{1}{(e^{\lambda_2} - e^{\lambda_1})}\left[N_7(e^{\lambda_1} - e^{\lambda_3}) + N_6(e^{\lambda_1} - e^{\lambda_4}) + \frac{R_e P_s}{\left(M^2 + \frac{1}{K}\right)}(e^{\lambda_1} - 1) - te^{\lambda_1}\right], \tag{A.12}$$

$$N_9 = N_6 + N_7 + N_8 + \frac{R_e P_s}{\left(M^2 + \frac{1}{K}\right)} - t, N_{10} = (e^{\lambda_5} - e^{\lambda_7})(\lambda_6^2 - \lambda_7^2), \tag{A.13}$$

$$N_{11} = (e^{\lambda_5} - e^{\lambda_8})(\lambda_6^2 - \lambda_8^2), \tag{A.14}$$

$$N_{12} = \frac{R_e P_O}{\left(M^2 + \frac{1}{K} + R_e i\omega\right)}(e^{\lambda_5} - 1)\lambda_6^2, \tag{A.15}$$

$$N_{13} = (\lambda_5^2 e^{\lambda_6} - \lambda_6^2 e^{\lambda_5})(\lambda_5^2 e^{\lambda_5} - \lambda_7^2 e^{\lambda_7}) - (\lambda_5^2 e^{\lambda_7} - \lambda_7^2 e^{\lambda_5})(\lambda_5^2 e^{\lambda_5} - \lambda_6^2 e^{\lambda_6}), \tag{A.16}$$

$$N_{14} = (\lambda_5^2 e^{\lambda_5} - \lambda_8^2 e^{\lambda_8})(\lambda_5^2 e^{\lambda_6} - \lambda_6^2 e^{\lambda_5}) - (\lambda_5^2 e^{\lambda_8} - \lambda_8^2 e^{\lambda_5})(\lambda_5^2 e^{\lambda_5} - \lambda_6^2 e^{\lambda_6}), \tag{A.17}$$

$$N_{15} = \frac{R_e \lambda_5^2 P_o}{\left(M^2 + \frac{1}{K} + R_e i\omega\right)}\left[e^{\lambda_5}(\lambda_5^2 e^{\lambda_6} - \lambda_6^2 e^{\lambda_5}) - (\lambda_5^2 e^{\lambda_5} - \lambda_6^2 e^{\lambda_6})\right], \tag{A.18}$$

$$N_{16} = \frac{N_{15} N_{10} - N_{12} N_{13}}{N_{11} N_{13} - N_{14} N_{10}}, N_{17} = \frac{N_{12} N_{14} - N_{11} N_{15}}{N_{11} N_{13} - N_{10} N_{14}}, \tag{A.19}$$

$$N_{18} = \frac{1}{(e^{\lambda_6} - e^{\lambda_5})}(N_{17}(e^{\lambda_5} - e^{\lambda_7}) + N_{16}(e^{\lambda_5} - e^{\lambda_8}) + \frac{R_e P_o}{\left(M^2 + \frac{1}{K} + R_e i\omega\right)}(e^{\lambda_5} - 1)), \tag{A.20}$$

$$N_{19} = N_{16} + N_{17} + N_{18} + \frac{R_e P_o}{\left(M^2 + \frac{1}{K} + R_e i\omega\right)}, \tag{A.21}$$